(13) Bendler, J. T.; Yaris, R. *Macromolecules* **1978**, *11*, 650.
(14) Fits of the data to the Williams–Watts function were overall not as successful as the GDL model. The Williams–Watts fits indicated that $\beta = 0.60 \pm 0.03$ over the concentration and temperature range studied.
(15) Wahl, P. *Biophys. Chem.* **1979**, *10*, 91.
(16) Bevington, P. R. *Data Reduction and Error Analysis for the Physical Sciences*; McGraw-Hill: New York, 1969; p 237.
(17) Nemoto, N.; Landry, M. R.; Noh, I.; Yu, H. *Polym. Commun.* **1984**, *15*, 141.
(18) Gotro, J. T.; Graessley, W. W. *Macromolecules* **1984**, *17*, 2767.
(19) Howarth, O. W. *J. Chem. Soc., Faraday Trans. 2* **1980**, *76*, 1219.
(20) Fytas, G.; Ngai, K. L. *Macromolecules* **1988**, *21*, 804. Alig, I.; Stieber, F.; Wartewig, S.; Fytas, G. *Polymer* **1988**, *29*, 975.
(21) Heatley, F. *Prog. Nucl. Magn. Reson. Spectrosc.* **1979**, *13*, 47.
(22) Hatada, K.; Kitayama, T.; Terakawi, Y.; Tanaka, Y.; Sato, H. *Polym. Bull. (Berlin)* **1980**, *2*, 791.
(23) Landry, M. R.; Gu, Q.; Yu, H. *Macromolecules* **1988**, *21*, 1158.
(24) Ferry, J. D. *Viscoelastic Properties of Polymers*; Wiley: New York, 1980; Chapters 11, 17.
(25) (a) Jones, A. A.; Robinson, G. C.; Gerr, F. E. *ACS Symp. Ser.* **1979**, *No. 103*, 271. (b) Komoroski, R. A.; Mandelkern, L. J. *J. Polm. Sci., Polym. Symp.* **1976**, *No. 54*, 227.
(26) Fujita, H. *Adv. Polm. Sci.* **1961**, *3*, 1. Fujita, H.; Kishimoto, A.; Matsumoto, K. *Trans. Faraday Soc.* **1960**, *56*, 424.
(27) von Meerwall, E. D.; Amis, E. J.; Ferry, J. D. *Macromolecules* **1985**, *18*, 260.
(28) von Meerwall, E. D.; Ferguson, R. D. *J. Appl. Polym. Sci.* **1979**, *23*, 877.
(29) See for example: Friedrich, C.; Laupretre, F.; Noel, C.; Monnerie, L. *Macromolecules* **1981**, *14*, 1119.
(30) Schaeffer, J. *Macromolecules* **1973**, *6*, 882.
(31) Weber, T. A.; Helfand, E. *J. Phys. Chem.* **1983**, *87*, 2881.

Molecular Dynamics Simulation of Polymer Liquid and Glass. 3. Chain Conformation

David Rigby and R. J. Roe*

Department of Materials Science and Engineering, University of Cincinnati, Cincinnati, Ohio 45221-0012. *Received August 1, 1988; Revised Manuscript Received November 7, 1988*

ABSTRACT: Molecular dynamics simulation has been performed with dense systems of alkane-like chain molecules subject to potentials restricting bond lengths, bond angles, and trans–gauche torsional angles and interacting with neighboring chains according to a truncated Lennard-Jones potential. The distributions of bond lengths, bond angles, and torsional angles have been evaluated for a range of density varying by a factor of 2. The overall population of trans conformer was found to be independent of density, in contrast to experimental results suggesting an enhancement of gauche conformer on densification of short-chain alkanes. A closer examination showed, however, that gauche enhancement occurred mainly among bonds at the chain ends and only at the high end of the density range studied. The nonbonded interaction energy was found to go through a minimum as the density was increased, and at densities higher than that corresponding to the potential energy minimum, the molecular shape was somewhat modified through reductions in the bond lengths and bond angles as well as the trans conformer populations. The conformer population over a temperature range sufficiently above the T_g is well reproduced by the rotational isomeric state model, provided an "effective" trans–gauche energy difference, rather than the true value of the parameter used for the simulation, is used for the prediction.

1. Introduction

In recent work[1,2] we have performed molecular dynamics simulations of short polymethylene chains in the bulk state and have found that, on cooling at constant pressure, the simulated systems undergo changes with features in common with glass-forming materials studied in the laboratory. In particular, one observes that over a fairly narrow temperature range, the temperature coefficients of density and internal energy undergo characteristic changes. This occurrence is preceded at slightly higher temperature by cessation of conformational changes and followed at lower temperature by a cessation of translational diffusion.[1] A subsequent study of short-range order in these supercooled liquid and glassy systems[2] showed that, on cooling, a local alignment of short sections of chains begins to develop and that the volume of the associated correlated regions appears to diverge at a temperature above the previously determined glass temperature. Annealing just below this temperature was found to produce a highly ordered, but noncrystalline, structure.

In the present work, in which we continue our program of evaluating detailed properties of the simulated system, we focus our attention on the conformational properties of the chain molecules in the bulk liquid state with respect to distribution of bond lengths, bond angles, and trans–gauche conformers. We investigate, in particular, the effect of densification on the chain conformation above the glass transition temperature.

Experimental evidence indicating that pressure densification enhances the population of gauche conformers was first reported by Schoen et al.[3a] from their Raman scattering studies on *n*-heptane subjected to pressures up to 14.7 kbar. In a later, more detailed study,[3b] these workers found the same trend in *n*-hexane and *n*-octane as well as, to a lesser degree, in *n*-hexadecane. The analysis of the *n*-heptane data also suggested that the populations of those conformers with only a single gauche bond decreased with increasing pressure, while those with 2–4 gauche bonds increased. These findings were contradicted by Schwickert et al.,[4] who reported their Raman measurements showing that, with the *n*-alkanes C_6, C_8 C_9, and C_{12} at pressures up to 6 kbar, various bands of interest narrowed but no change in integral intensities was observable. The subsequent Raman measurements by Wong et al.,[5] however, confirmed the earlier conclusions of Schoen et al.,[3] showing a decrease in the overall trans population with increasing pressure, although in this case the population of both the single and double gauche forms exhibited the same pressure dependence.

A pressure densification effect on conformer population was found also in the Monte Carlo simulation of *n*-butane by Jorgensen.[6] The simulation, run at pressures of 1, 5000,

0024-9297/89/2222-2259$01.50/0

Table I
Constants Used for Potential Functions

	in reduced units	in absolute units
l_0	0.4	0.152 nm
cos θ_0	−0.3333	−0.3333
k_b	10^4	3.46×10^7 J·nm^{-2}·mol^{-1}
k_θ	10^3	5×10^5 J·mol^{-1}
k_ϕ	18	9000 J·mol^{-1}
a_0	1	1
a_1	1.3100	1.3100
a_2	−1.4140	−1.4140
a_3	−0.3297	−0.3297
a_4	2.8280	2.8280
a_5	−3.3943	−3.3943
$\Delta E_{t\to g}$	5.68	2842 J·mol^{-1}
trans–gauche barrier ($\phi = \pm 60°$)	23.96	11 978 J·mol^{-1}
cis barrier ($\phi = 180°$)	86.89	43 444 J·mol^{-1}

and 15 000 atm and at a temperature of −0.5 °C, revealed that the trans population decreased slightly from 67.8 to 66.4% between 1 and 5000 atm, with a slightly larger rate of decrease to 61.7% between 5000 and 15 000 atm.

2. Chain Model and Method

As described in our previous publication,[1] chains are modeled as sequences of CH_2 segments connected by springlike backbone bonds and with additional potentials controlling bond angles and torsional motions. A truncated Lennard-Jones 6–12 potential is used to represent nonbonded interactions between segments in different chains and between segments separated by more than three bonds along the same chain. Contributions to the potential energy of the system from the four sources described above have the following forms:

$$E_{b,j} = (1/2)k_b(l_j - l_0)^2 \tag{1}$$

$$E_{\theta,j} = (1/2)k_\theta(\cos\theta_j - \cos\theta_0)^2 \tag{2}$$

$$E_{\phi,j} = k_\phi \sum_{n=0}^{5} a_n \cos^n \phi_j \tag{3}$$

$$E_{nb,ij} = 4\epsilon^*\left[\left(\frac{r^*}{r_{ij}}\right)^{12} - \left(\frac{r^*}{r_{ij}}\right)^{6}\right] + \text{constant} \qquad \text{for } r_{ij} \le 1.5r^* \tag{4}$$

and

$$E_{nb,ij} = 0 \qquad \text{for } r_{ij} > 1.5r^*$$

The actual constants used in eq 1–4 are listed in Table I. The system simulated consists of a cubic box containing 500 or 2000 CH_2 units and subject to a periodic boundary condition. The larger system was used for chains with more than 20 segments to ensure that a molecule does not interact with its own image. The equations of motion were integrated for each segment numerically using the Verlet algorithm.[7] Details of the computational procedures are described fully in ref 1.

For convenience, we use a set of reduced units in which the unit of mass corresponds to the mass of a CH_2 group, and the units of length and energy were given by the Lennard-Jones length and energy parameters, respectively. Values of these parameters appropriate for polymethylene and other reduced units derived therefrom are listed in Table II.

Simulations aimed at investigating the densification effect were performed at reduced temperatures T equal to 4.0 and 6.0 for chains with 10 and 20 CH_2 units. In all cases, systems were first equilibrated at densities corresponding to the pressure p equal to 3.0 reduced units. Compression in steps of 0.04 or 0.05 reduced density units (achieved by isotropically scaling all distances) was performed until a density of 2.0 was reached; thereafter, compression in smaller steps of 0.02 or 0.025 reduced density units followed. The duration of a simulation between compression steps was typically 5000 integration steps at the lower densities and 10 000 steps above $\rho = 2.0$. At selected densities much longer

Table II
Scaling Parameters Used for Expressing Quantities in Reduced Units

energy ϵ^*	500 J·mol^{-1}
length r^*	0.38 nm
mass m	14 g·mol^{-1}
temperature $T^* = \epsilon^*/k$	60.1 K
pressure $p^* = \epsilon^*/r^{*3}$	15.16 MPa (0.1516 kbar)
time $\tau^* = (mr^{*2}/\epsilon^*)^{1/2}$	2.01 ps
density $\rho^* = 1/r^{*3}$	18.22 nm^{-3} (0.424 g·cm^{-3})

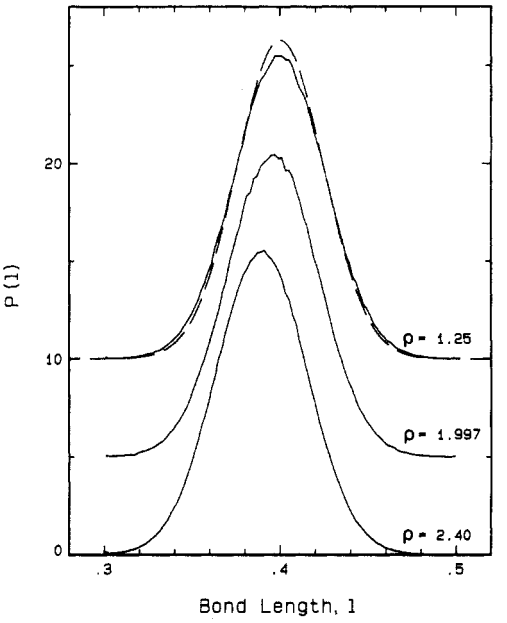

Figure 1. Distribution of bond lengths at densities of 1.25, 1.997, and 2.40 during densification at $T = 6$. The three curves are displaced vertically from each other for legibility. The dashed curve was obtained from the Boltzmann factor $\exp(-V/kT)$, where V denotes the bond-stretching potential.

simulation runs were carried out for the purpose of analyzing the conformer population. Rotational states trans, gauche$^+$, and gauche$^-$ were assigned to those bonds having dihedral angles in the range −60 to +60°, +60 to +180°, and −180 to −60°, respectively. In general, conformations were analyzed at every tenth integration step, and the simulation continued for the duration of between 20 000 and 60 000 integration steps until the populations of g^+ and g^- conformers agreed within 0.5–0.8% of each other. In a further attempt to establish the accuracy of conformer populations, the system of 10-segment chains at $T = 4$, having been compressed to a density of 2.132, was heated in a single step to $T = 6$ and allowed to reequilibrate at this temperature. The conformer populations thus evaluated were found to agree well with those measured with the system, which had been maintained at $T = 6$ throughout. A similarly good agreement was found when the $T = 6$ system was suddenly quenched to $T = 4$.

3. Results and Discussion

Figures 1–3 show the distributions of bond lengths, valence angles, and torsional angles evaluated for the system of 10-segment chains at reduced temperature T equal to 6.0 and at reduced densities ρ equal to 1.25, 1.997, and 2.4. The three curves in each figure are displaced vertically from each other for legibility. Superimposed on the curve for $\rho = 1.25$ in each figure is the dotted curve, which was calculated from the Boltzmann factor $\exp(-V/kT)$ where V is the potential energy restricting the bond length, bond angle, and torsional angle, as represented by eq 1–3, respectively. At relatively low densities, $\rho = 1.25$ and 1.997, the distribution of bond lengths and bond angles differs very little from the Boltzmann distribution, indicating that the restrictions imposed by the space-filling requirements in segment packing are still not severe enough to alter these

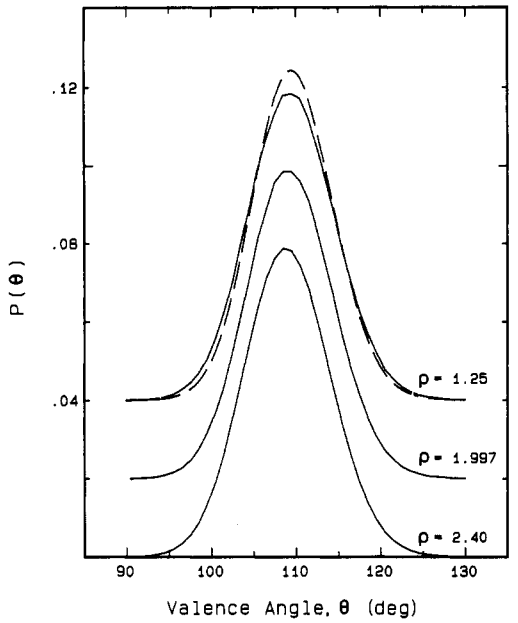

Figure 2. Distribution of valence angles during densification at $T = 6$, for the same densities as in Figure 1. The dashed curve was computed from the Boltzmann factor for the bond angle bending potential. Note that the maximum has shifted slightly toward lower angle at the highest density.

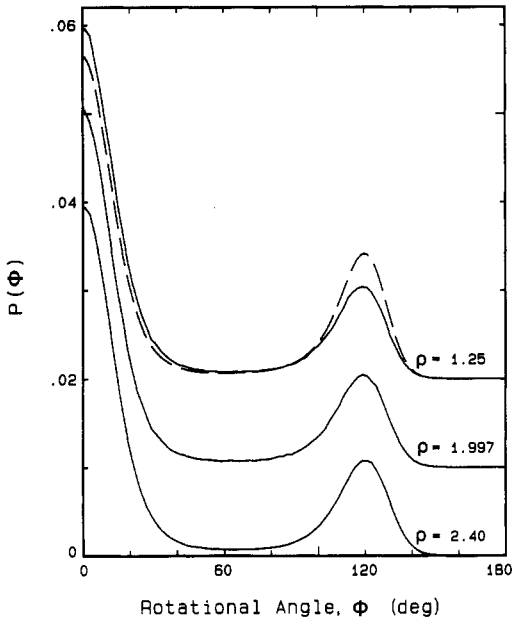

Figure 3. Torsional angle distributions for the same cases shown in Figures 1 and 2.

distributions. At the higher density, $\rho = 2.40$, the most probable bond length and bond angles have decreased by about 0.01 reduced length and about 1°, respectively. (Please note that the change in bond length is exaggerated because of the use of a bond spring constant, which is much weaker than a realistic model value; see ref 1.)

In Figure 3, it is seen that, even at the low density $\rho = 1.25$, the distribution of torsional angles deviates from the Boltzmann distribution, which in effect is the value predicted for individual isolated bonds. The substantial suppression of gauche isomers in the simulated results arises from the interaction of neighboring bonds leading to exclusion of g^+g^- sequences. The result in Figure 3 is in conflict with similar results published previously by other workers. Avitabile and Tuzi[8] performed Monte Carlo simulation of a model of the alkane C_{24} in which a CH_2 group is represented by a single spherical segment and the

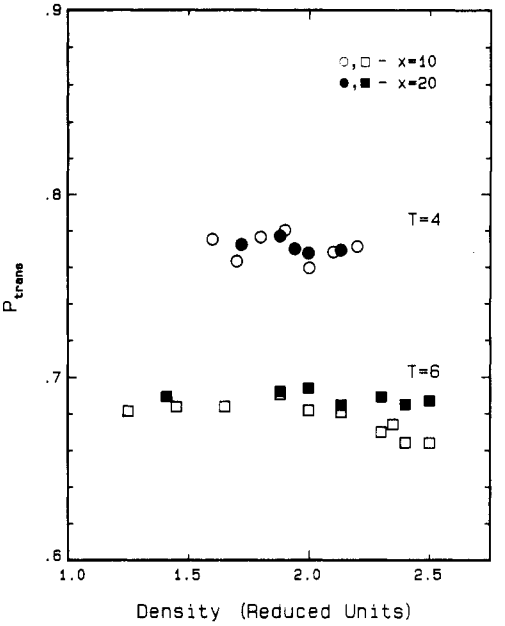

Figure 4. Overall trans fractions for chains with 10 and 20 segments at temperatures of 4 and 6 reduced units: ○, $x = 10$, $T = 4$; □, $x = 10$, $T = 6$; ●, $x = 20$, $T = 4$; ■, $x = 20$, $T = 6$.

bond length and bond angle are rigidly fixed. The distribution of torsional angles they obtained from the simulations shows an enhancement of population in the high potential energy region (with corresponding reduction in the trans and gauche maxima heights) and the shift of the most probable gauche angles toward the trans by a few degrees. It is difficult to see the reason for the discrepancy from our results, but we may note that others[9] have pointed out the fact that a rigid constraint for the bond angle in the model can affect the dynamic behavior of torsional motion of chain molecules.

The three simulation results at $\rho = 1.25$, 1.997, and 2.40 show that densification has no recognizable effect on the distribution of torsional angles. In Figure 4, we plot the fractional population of trans conformers as a function of density for chains with 10 and 20 segments at temperatures T of 4.0 and 6.0 reduced units (ca. 240 and 361 K), confirming that, within the experimental error, no major change in the conformer population occurs as the density is increased. This is an unexpected result on the face of the rather strong experimental evidence (and the Monte Carlo simulation results of Jorgensen[6]), suggesting the enhancement of gauche conformers with pressure densification. In view of the conflicting experimental observations concerning the behavior of sequences of gauche bonds mentioned in the introduction, Figure 5 illustrates the populations of various three-bond sequences ttt, (ttg^+, ttg^-, g^+tt, g^-tt), (tg^+t, tg^-t), and (g^+tg^+, g^+tg^-, g^-tg^-, g^-tg^+). Here again, no significant pressure effect can be observed for any of the sequences, with the possible exception of the ttt sequence in chains of 10 segments at high densities.

The fact that most of the experimental evidence on the gauche enhancement on densification was obtained with short alkane chains suggests an investigation of the role played by the chain ends. We therefore classify the bonds into terminal bonds (i.e., bonds penultimate to the terminal CH_3 segments) and internal bonds, and the populations of trans bonds belonging to these two separate groups (for chains of 10 segments at $T = 6.0$) are plotted in Figure 6. This shows that, while the trans probability for the internal bonds remains essentially constant on densification, the trans probability for the terminal bonds decreases steadily beyond the density of about 2.0 reduced units. The dif-

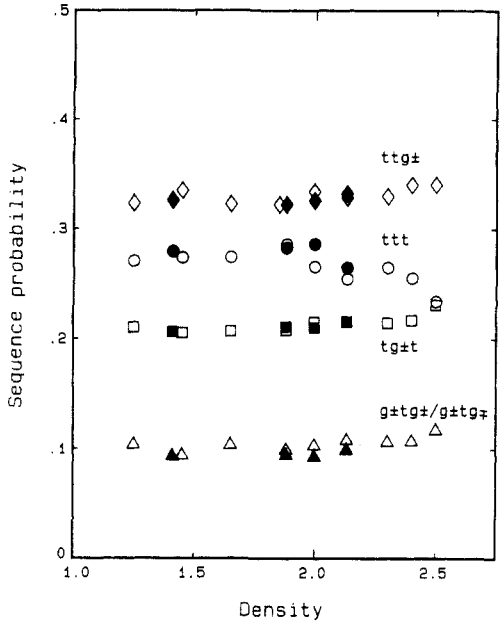

Figure 5. Probabilities of various three-bond rotational angle sequences for chains with 10 and 20 segments at $T = 6$. Filled symbols are for $x = 20$.

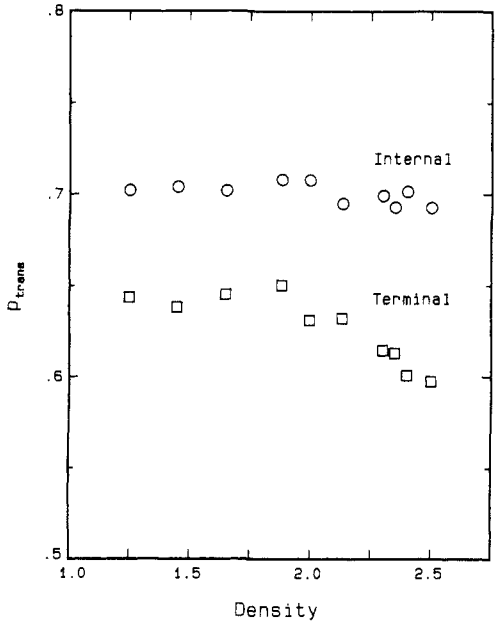

Figure 6. Trans fractions plotted separately for internal and terminal torsional angles, in the chain with 10 segments at $T = 6$: ○, internal bonds; □, terminal bonds.

ferences between the terminal and internal bonds arise only with respect to the torsional angle distribution. When the distributions of bond lengths and bond angles are plotted separately for internal and terminal bonds, the curves obtained show no recognizable difference. Note also that while the total population of conformers with a terminal trans bond decreases on densification, the effects on individual conformers may be more complex. For example, a detailed examination of three-bond sequences for the $x = 10$, $T = 6$ case shows that all sequences with a gauche bond at the chain end either increase in population ($ttg^{\pm}$, $g^{\pm}tg^{\pm}$, $g^{\pm}tg^{\mp}$) or are unchanged ($tg^{\pm}g^{\pm}$, $g^{\pm}g^{\pm}g^{\pm}$). Sequences with a trans terminal bond either decrease in population (ttt, $g^{\pm}g^{\pm}t$), are unchanged ($g^{\pm}tt$), or may even increase ($tg^{\pm}t$). However, the large decrease of 6% in the ttt population is offset only slightly by the 1.5% increase associated with $tg^{\pm}t$.

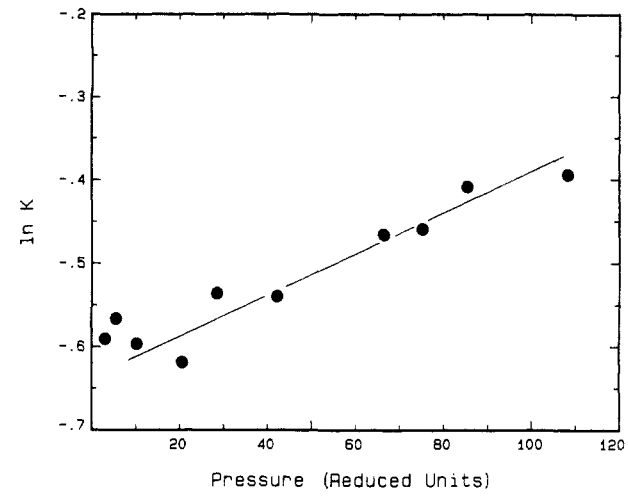

Figure 7. Pressure dependence of the equilibrium constant for conversion of trans- to gauche-terminated chains.

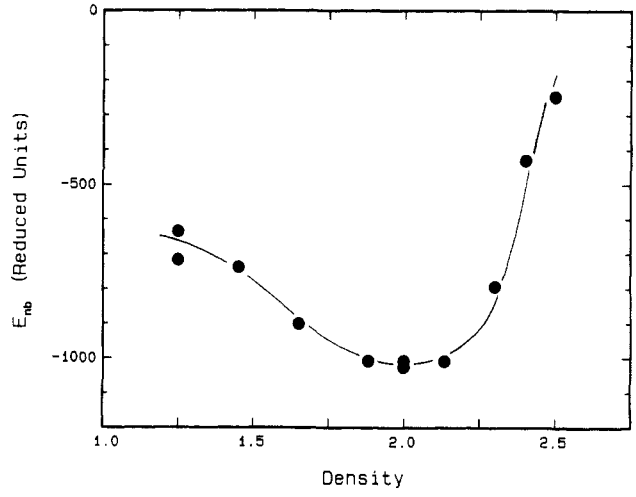

Figure 8. Nonbonded portion of the potential energy as a function of density for the $x = 10$ system at $T = 6$. The two sets of data at $\rho = 1.25$ and 1.997 were obtained during sequential simulation runs at these temperatures.

The shift in the terminal bond conformer populations with density can be attributed to an apparent difference in the volumes of the conformers. The volume differences Δv between chains with and without terminal gauche bonds can be evaluated from

$$-\Delta v = kT(\partial \ln K/\partial p)_T \quad (5)$$

where K denotes the equilibrium constant for the transformation between chain conformers with a terminal gauche state and trans state and can be equated to $(1 - P_t)/P_t$, P_t being the fractional trans population. The resulting plot of $\ln K$ vs p at $T = 6.0$ is illustrated in Figure 7, from which we obtain

$$\begin{aligned}\Delta v &= -0.0145 \pm 0.003 \text{ reduced volume units} \\ &= -0.795 \text{ Å}^3 \\ &= -0.48 \text{ cm}^3/\text{mol}\end{aligned} \quad (6)$$

This value compares favorably with the value of −0.4 cm^3/mol estimated by Jorgensen from his Monte Carlo simulation on n-butane.[6] Compared with experimental data, however, it is clearly smaller than the value of −2 cm^3/mol estimated for n-hexane by Pratt et al.[10] and the value of −1.1 cm^3/mol given by Wong et al.[5] Values for a variety of simple compounds also lie typically in the range −1 to −4 cm^3/mol.[11]

The contribution to the total potential energy of the system by the nonbonded interaction, according to the

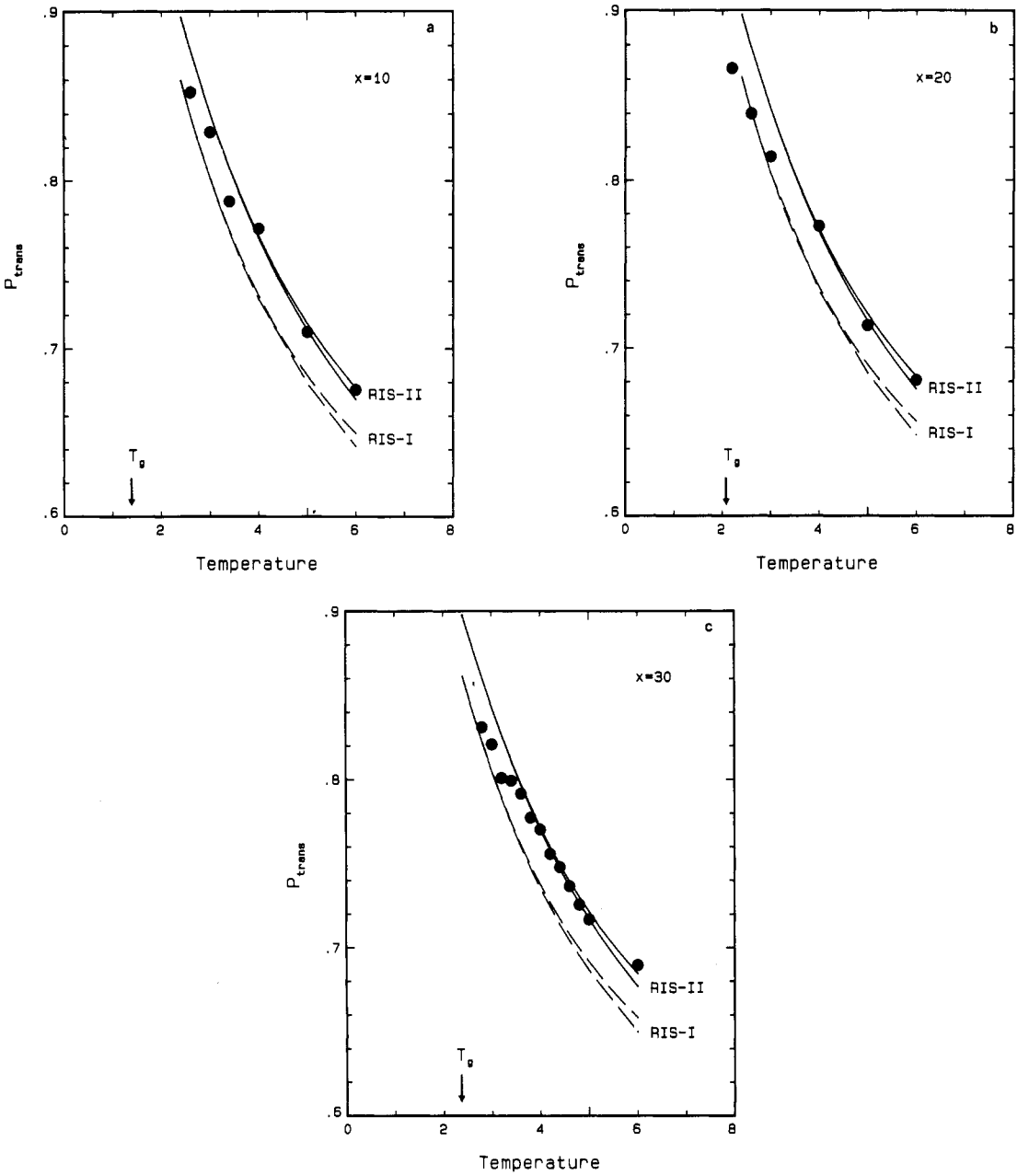

Figure 9. Temperature dependence of the overall trans conformer populations for chains with (a) 10, (b) 20, and (c) 30 segments at densities corresponding to a pressure of 3 reduced units. RIS-I curves are for RIS model with the same trans–gauche energy difference as the torsional potential used in the simulation (679.3 cal·mol^{-1}). RIS-II curves obtained using a best value of 790 cal·mol^{-1} as required to fit the simulation data. (Upper curve of each set refers to E_ω = 2500 cal·mol^{-1}; lower curve refers to E_ω = 1500 cal·mol^{-1}.)

Lennard-Jones potential, is plotted in Figure 8 against density. It is seen that the nonbonded potential energy goes through a distinct minimum at about ρ = 2.0. The contributions to the potential energy from other sources, i.e., bond length stretching, bond angle bending, and bond torsion, show only a moderate variation through the density range considered, so that the plot of total potential energy against density shows a similar minimum at ρ = 2.0. We note that in Figures 1 and 2 changes in the most probable bond length and bond angle become recognizable beyond ρ = 2.0, and also in Figure 6 the decrease in the trans population of terminal bond begins around ρ = 2.0. It thus appears that moderate densification (ρ < 2.0) brings about improvement in the segmental packing, thus lowering the nonbonded potential energy but without distorting the molecular shape in any way. Further densification (ρ > 2.0) evidently forces segments closer together against the repulsive part of the nonbonded potential, even inducing modifications to the molecular shape itself as revealed by changes in the bond length, bond angle, and torsional angle. The shortening of the bond length, which amounts to a decrease in the atomic radius on densification, is understandable. Why the bond angle should decrease from the tetrahedral angle of 109° is not easily explainable. One may also wonder whether the decrease in the bond angle will be realized even when the model explicitly recognizes the two hydrogens attached to the carbon atoms. When the distribution of torsional angle of only the terminal bonds, evaluated at ρ = 2.4, is superposed on the plot in Figure 3, it is seen that, aside from the enhancement of the height of the gauche peak, there is no change in either the peak position or the shape of the gauche and trans peaks. Hence, the effect of densification is simply to modify the trans–gauche populations. The analysis described above, based on the data in Figure 7, leads to the conclusion that the molecules having a penultimate gauche bond has a volume smaller by 0.795 Å^3 compared to those having a terminal trans bond. Evi-

dently, a penultimate gauche bond affords a more compact molecular shape, but a visualization of a reduction of nearly 1 Å^3 in molecular volume by means of mechanical molecular models is not easily achieved.

With the exception of the end effect, the results described above show the conformer population is essentially unaffected by pressure densification. Even the gauche enhancement of penultimate bonds becomes noticeable only at densities in absolute units greater than 0.9 g/cm^3 for 10-segment chains and 1.0 g/cm^3 for 20 segment chains, which are realized at pressures greater than ca. 5.0 kbar.[12] Accordingly, for most purposes, the statistical characteristics of chain conformation should be considered a function of temperature only. Figure 9 shows the temperature dependence of trans conformer population for chains with 10, 20, and 30 segments (evaluated during stepwise cooling/compression runs at constant average pressure of 3.0 reduced units). These simulation results are compared with the prediction from the rotational isomeric state model. The pair of dashed line curves in each figure was obtained with the parameter E_σ taken equal to the trans-gauche energy difference 679.3 cal/mol used in the torsional potential energy function for the simulation and with the E_ω values equal to 1500 and 2500 cal/mol, which represent the range of values normally quoted for this parameter. The solid lines were calculated with a value of E_σ equal to 790 cal/mol and E_ω again equal to either 1500 or 2500 cal/mol. The dashed lines, calculated with the use of the "true" trans-gauche energy difference, fail to reproduce the conformer population correctly, but the solid lines calculated with the use of "effective" energy difference are able to represent the population faithfully at temperatures greater than 3.5 reduced units. The rotational isomeric state model in effect neglects all intermolecular interactions and all intramolecular interactions beyond those involving a four-bond sequence. Despite such simplification, it is gratifying to see that the model is capable of predicting the conformer populations correctly, provided a suitably adjusted numerical value is used to represent the effective trans-gauche energy difference.

Acknowledgment. This work has been supported in part by NSF Grant DMR8520921.

References and Notes

(1) Rigby, D.; Roe, R. J. *J. Chem. Phys.* **1987**, *87*, 7285.
(2) Rigby, D.; Roe, R. J. *J. Chem. Phys.* **1988**, *89*, 5280.
(3) (a) Schoen, P. E.; Priest, R. G.; Sheridan, J. P.; Schnur, J. M. *Nature (London)* **1977**, *270*, 412. (b) *J. Chem. Phys.* **1979**, *71*, 317.
(4) Schwickert, H.; Strobl, G. R.; Eckel, R. *Colloid Polym. Sci.* **1982**, *260*, 588.
(5) Wong, P. T. T.; Mantsch, H. H.; Snyder, R. G. *J. Chem. Phys.* **1983**, *79*, 2369.
(6) Jorgensen, W. L. *J. Am. Chem. Soc.* **1981**, *103*, 4721.
(7) Verlet, L. *Phys. Rev.* **1967**, *159*, 98.
(8) Avitabile, G.; Tuzi, A. *J. Polym. Sci., Polym. Phys. Ed.* **1983**, *21*, 2379.
(9) van Gunsteren, W. F.; Karplus, M. *Macromolecules* **1982**, *15*, 1528.
(10) Pratt, L. R.; Hsu, C. S.; Chandler, D. *J. Chem. Phys.* **1978**, *68*, 4202.
(11) Taniguchi, Y. *J. Mol. Struct.* **1985**, *126*, 241.
(12) For the purpose of comparison with experiment, pressures measured in the simulation have here been corrected for the effect of truncation of the nonbonded potential using standard procedures (see, e.g., ref 7) and assuming that the nontruncated potential adequately describes the actual nonbonded interactions.

Volumetric Behavior of Glassy Polymer-Penetrant Systems

J. S. Vrentas* and C. M. Vrentas

Department of Chemical Engineering, The Pennsylvania State University, University Park, Pennsylvania 16802. *Received June 21, 1988; Revised Manuscript Received October 17, 1988*

ABSTRACT: A model is proposed for predicting the volumetric behavior of the glassy polycarbonate-carbon dioxide system. This model is based on the hypothesis that the molecular structure of a glassy polymer changes with changing penetrant concentration. The predictions of the model are in reasonably good agreement with experimental data.

Introduction

When a low molecular weight penetrant is added to a polymer melt, the volume of the mixture at a particular temperature can be determined by using the following equation, if volume change on mixing effects are negligible:

$$\frac{V_m}{V_0} = \frac{\omega_1}{1-\omega_1}\frac{\hat{V}_1^0}{\hat{V}_2^0} + 1 \qquad (1)$$

Here, V_m is the total volume of the mixture, V_0 is the volume of the pure polymer, ω_1 is the mass fraction of penetrant, $\hat{V}_1^0$ is the specific volume of the pure penetrant, and $\hat{V}_2^0$ is the specific volume of the pure equilibrium liquid polymer. If a penetrant is added to a glassy polymer, it would appear reasonable to suppose that the volume of the system could be determined by using the following relationship:

$$\frac{V_m}{V_0} = \frac{\omega_1}{1-\omega_1}\frac{\hat{V}_1^0}{\hat{V}_{2g}^0(\omega_1=0)} + 1 \qquad (2)$$

Here, $\hat{V}_{2g}^0(\omega_1=0)$ is the specific volume of the pure glassy polymer which would be used in volumetric calculations in the limit of zero penetrant concentration. It has been suggested,[1] however, that eq 2 can seriously overestimate the volume of the mixture, and consequently, it has been postulated that only a fraction of the penetrant leads to volume dilation for a glassy polymer-penetrant system. The rest of the penetrant molecules participate in a hole-filling process and thus do not contribute to any volume expansion. This so-called dual mode sorption model distinguishes between dissolved penetrant and penetrant which is used to fill gaps in the polymer matrix.

The purpose of this paper is to propose an alternative explanation for the volumetric behavior of glassy poly-

0024-9297/89/2222-2264$01.50/0